Proceedings of the 20th International Conference on Soil Mechanics and Geotechnical Engineering– Rahman and Jaksa (Eds)

Experimental study on seismic deformation modes of steel-strip reinforced earth wall induced by segmental wall panels

Etude expérimentale sur les modes de déformation sismique d'un mur en terre armée de feuillards d'acier induits par des panneaux muraux segmentés

Yuusuke Miyazaki, Yasuo Sawamura
Department of Urban Management, Kyoto University, Japan, miyazaki.yusuke.6w@kyoto-u.ac.jp

Jotaro Ito, Makoto Kimura
Department of Civil and Earth Resources Engineering, Kyoto University, Japan

ABSTRACT: The current design method for steel-strip reinforced earth walls considers the mechanical role of the wall structure as a simple rigid structure. However, this consideration is likely to ruin the safety of the external stability against the sliding, overturning, and bearing capacity of the reinforced earth walls. In this study, therefore, dynamic centrifuge tests were conducted on a steel-strip reinforced earth wall with a modeled segmental wall structure. In addition, the results of the tests were compared with the results of centrifuge tests on a continuous wall model. It was found that, even if there was no shear resistance or bending resistance in the wall structure, the overall wall deformation mode in the segmental wall model exhibited similar results to those of the continuous wall model. On the other hand, the segmental wall model exhibited discontinuous wall displacements. They were induced by the independent mechanical behavior of each segmental wall panel. This independent mechanical behavior seems to have been caused by the different relationships among the confining stress, tensile force of the steel-strips, and wall displacement at each height of the segmental wall panels.

RÉSUMÉ : La méthode actuelle de conception des murs en terre renforcée par des bandes d'acier considère le rôle mécanique de la structure du mur comme une simple structure rigide. Cette considération est susceptible de ruiner la sécurité de la stabilité externe contre le glissement, le renversement, et la capacité de charge des murs en terre renforcée. Dans cette étude, donc, des essais dynamiques de centrifugation ont été effectués sur un mur en terre renforcée par des bandes d'acier avec une structure de mur segmentaire modélisée. En outre, les résultats des essais ont été comparés aux résultats des essais de centrifugation sur un modèle de mur continu. Même s'il n'y a pas de résistance au cisaillement ou à la flexion dans la structure du mur, le mode de déformation global du mur dans le modèle de mur segmentaire présente des résultats similaires à ceux du modèle de mur continu. D'autre part, le modèle de paroi segmentaire présente des déplacements de paroi discontinus. Ils ont été induits par le comportement mécanique indépendant de chaque paroi segmentaire. Ce comportement mécanique indépendant semble avoir été causé par des relations différentes entre la contrainte de confinement, la force de traction des bandes d'acier, et le déplacement de la paroi dans chaque hauteur de panneaux de paroi segmentaire.

KEYWORDS: steel-strip reinforced earth wall, segmental wall panel, geotechnical centrifuge, dynamic test, seismic mode

1 INTRODUCTION

The current design method for reinforced earth walls (REWs) does not take into account the mechanical effect of the multi-segmental wall structure. In a steel-strip REW, the stability of the vertical wall is maintained by the frictional force acting on the steel-strips as a reinforcement placed behind the wall facing, called concrete skin (Public Works Research Institute (PWRI), 2014). REWs are composed of many of these multi-segmental concrete skin panels. Even though it has been experimentally confirmed that there is a difference in the modes of wall deformation during earthquakes in multi-anchored retaining walls between the continuous facing type and the discontinuous facing type (Ichikawa et al., 2006), the seismic effect of the segmental wall panels on the wall deformation in REWs is unclear.

Tatsuoka (1992) classified the mechanical effects, in accordance with the wall stiffness, as shown in Figure 1. Based on this classification, a steel-strip REW seems to be located between Type C and Type D. This is because the segmental wall panels are connected to each other by steel bars. However, as shown in Figure 2, in the inspection process of the external stability where the sliding, overturning, and supporting of the REW are verified, the reinforced area and the walls are considered as a single earthwork structure. Therefore, the design

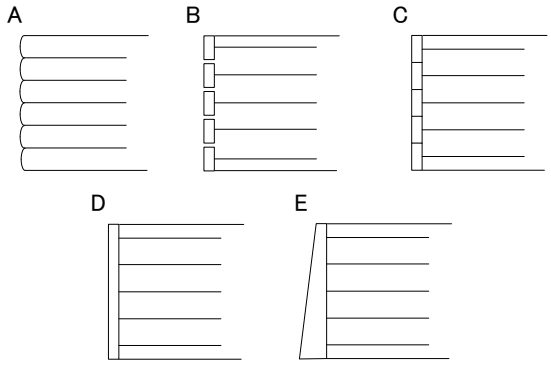

Type of wall	A	B	C	D	E
Local stiffness	×	○	○	○	○
Total shear stiffness	×	×	○	○	○
Total bending stiffness	×	×	×	○	○
Shear resistance due to self-weight	×	×	×	×	○

Figure 1. Mechanical effect due to wall structure (Modified after Tatsuoka, 1992).

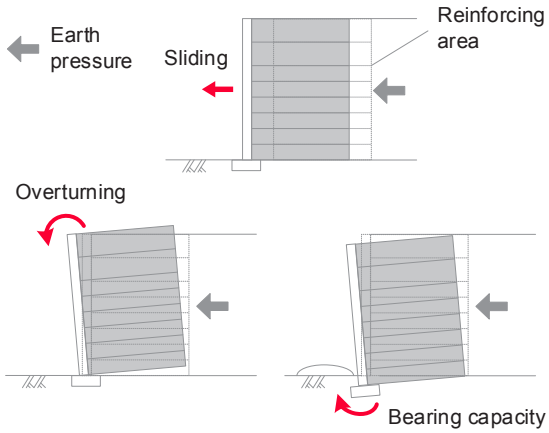

Figure 2. External stability in reinforced earth wall (Modified after PWRI, 2014).

of REWs is likely to be dangerous because there is a discrepancy between the assumed deformation mode in the design phase and the possible, flexible deformation mode that can actually occur in the segmental wall panels.

Therefore, the relationship between the segmental wall structure and the seismic behavior of steel-strip REWs must be clarified for rationalization in the seismic design. In this study, dynamic centrifuge model tests were conducted to confirm the seismic behavior of a steel-strip REW with segmental wall panels.

To compare the seismic behavior of a continuous wall with that of segmental wall panels, the experimental conditions of the present study were based on the past centrifuge model experiment by Sawamura et al. (2019). They used a steel-strip REW model with a non-segmental aluminum wall model which followed the current design concept in the investigation of the external stability. In the present experiment, a steel-strip REW model was used that simulates a Type B wall structure (Figure 1) without total shear or total bending stiffness.

2 OVERVIEW OF PHYSICAL MODELING

In this experiment, a centrifugal loading device, owned by the Disaster Prevention Research Institute of Kyoto University, was used. For the test conditions of a steel-strip REW with a non-segmental aluminum wall model, refer to Sawamura et al. (2019). The experimental conditions for the segmental wall model are summarized in the following.

2.1 *Experimental subjects and measurement items*

Figure 3 provides schematic diagrams of the experimental model with the non-segmental aluminum wall model (Case-1) and the segmental wall panels (Case-2). Figure 4 captures the experimental setup used in the wall model, reinforcement, and measuring instruments before the banking process in Case-2. The measured items were the response acceleration of the wall and the ground, the horizontal displacement of the wall, the horizontal earth pressure acting on the wall, and the strain generated in the reinforcement.

As mentioned below, a multi-segmental wall model was used, in which the wall was divided into sections at each height of the reinforcement. To keep the boundary conditions between the wall panels clear, Teflon sheets were attached to the upper and lower surfaces of the segmental wall panels, so that almost no friction would be expected to occur between them.

Thus, the total shear stiffness of the wall was small, and there was concern that the segmental wall panel at the top, where the confining pressure was quite small, might be pulled out during shaking. Therefore, it was decided that a small embankment

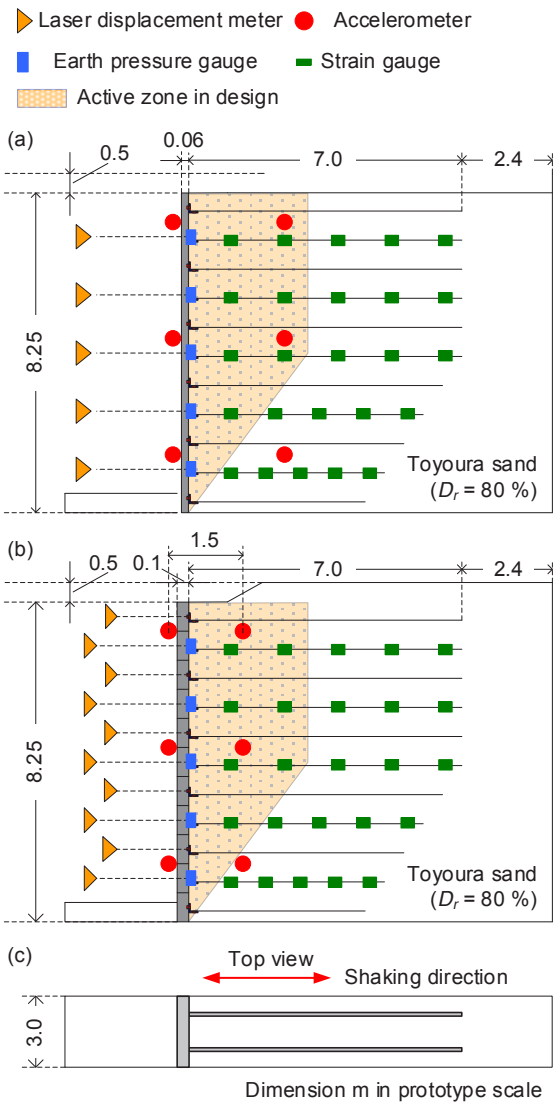

Figure 3. Schematic drawing and measurement instrumentation: (a) Case-1 (Modified after Sawamura et al., 2019), (b) Case-2, and (c) top view of models.

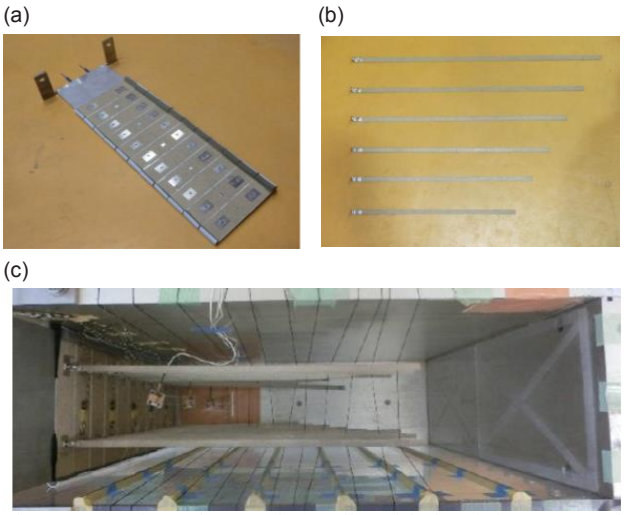

Figure 4. Experimental setup of (a) wall model, (b) reinforcement, and (c) arrangement of measuring instrument before banking (Black strings were used to support the horizontality of the reinforcements under air pluviation.).

would be constructed in the reinforced earth model in order to prevent the sudden pulling out of the top wall panel; no change in the design reinforcement length resulted from this construction. The dimensions of the embankment were a slope of 30º and a height of 0.5 m, starting from a position 1.0 m away from the wall in the prototype scale. The slope gradient was determined by considering the internal friction angle of the Toyoura sand. The overburden pressure due to the additional small embankment was 7.8 kPa in the prototype scale.

2.2 *Model ground and soil chamber boundaries*

Dry Toyoura sand was used to produce a uniform dry ground with a relative density of 80% by the air pluviation method at an adjusted falling height. The bottom of the sand chamber was treated as the foundation ground with sufficient strength.

The dynamic tests were conducted in a rigid soil chamber with a width of 630 mm, a height of 500 mm, and a depth of 150 mm. A gel sheet, with a thickness of 2.0 mm and a compressive strength of 0.07 N/mm^2 at 10% compression, was attached to the wall of the soil chamber as buffer material. The wall with the gel sheet was placed perpendicular to the direction of shaking to mitigate the effect of the soil chamber boundary. Additionally, in order to reduce the friction between the soil chamber's walls parallel to the shaking direction and the wall model, sponges with Teflon sheets were placed on both sides of the wall model.

2.3 *Modeling of segmental wall panels*

Figure 5 exhibits a schematic diagram of the segmental wall model. The material for the wall in this experiment was a wide rectangular aluminum block with a height of 36.5 mm, a width of 140 mm, and a thickness of 5.0 mm, instead of the complicated cross shape of real structures described in Figure 6, to simplify its modeling. The thickness of the wall material was determined so that the wall material itself would not be deformed by earth pressure. The height of the wall was determined so that the density of the reinforcement for the ground in each wall block would be the same as that of a real structure. As mentioned previously, to reduce the friction between the wall materials, 0.5-mm-thick Teflon sheets were attached to the top and bottom surfaces of the segmental wall panels.

In this way, the stiffness of the molded wall structure was reproduced by stacking 11 layers of these segmental wall panels, corresponding to Type B (see Figure 1); overall shear and bending resistance were not expected. Table 1 provides a comparison of the physical properties between the real objective structure and the model. On the other hand, to improve the adhesion between the segmental wall panels and the embankment, double-sided tape was attached to the surfaces of the segmental wall panels, and Toyoura sand was affixed to the surface of the double-sided tape toward the embankment.

2.4 *Modeling of reinforcement*

According to the manual for the design and construction of REWs with steel-strip reinforcement (PWRI, 2014), the standard friction angle between the embankment and the reinforcement should be more than 36º if the embankment material is good for compaction. Therefore, direct shear tests using Toyoura sand were conducted to select the reinforcement material for this experiment. To simulate the shearing behavior between Toyoura sand and the reinforcement, double-sided tape was attached to a stainless-steel base and the surface of the tape was coated with dry Toyoura sand. In this way, the shearing behavior between the frictional stainless-steel base, as a semi-reinforcement, and the Toyoura sand could be examined.

Figure 7 presents the results of the direct shear tests on Toyoura sand and Toyoura sand with the semi-reinforcement. Cohesion c = 5.0 kN/m^2 and internal friction angle ϕ = 37.3º were

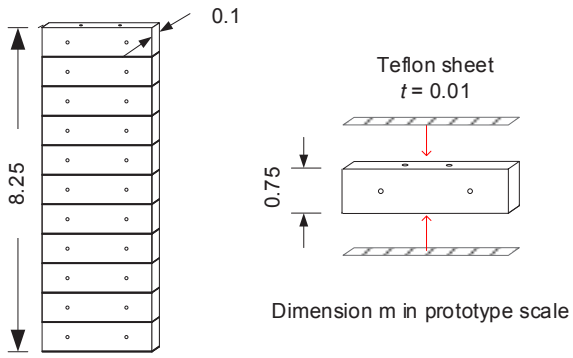

Figure 5. Schematic drawing of wall model.

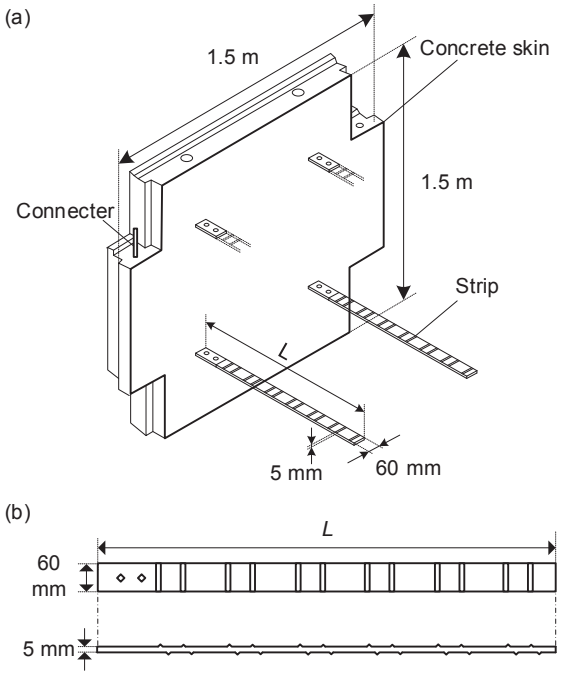

Figure 6. Schematic drawing of facing and strip in reinforced earth wall (Modified after PWRI, 2014). *L* means the length of reinforcement.

Table 1. Comparison of properties of wall structure between real structure and model.

	Object	Model
Young's modulus: E [kN/m^2]	2.40×107	7.03×107
Height: H [m]	1.50	8.25
Width: b [m]	1.50	2.80
Thickness: d [m]	0.18	0.06
Cross-sectional area: A [m^2]	2.25	23.1
Moment of area: I [m^4]	7.29×10-4	5.04×10-5
Axial stiffness: EA [kN]	5.40×107	1.62×109
Bending stiffness: EI [kN·m^2]	1.75×104	3.54×103

obtained in the tests between Toyoura sand and the semi-reinforcement. This indicates that the cohesive force between the semi-reinforcement and the Toyoura sand matched the reinforcing principle and satisfied the standard friction angle specified in the design. Therefore, stainless-steel coated with Toyoura sand was used as the material for the reinforcement.

Table 2 provides a comparison of the physical properties between the reinforcement model and the real objective reinforcement.

The design of a steel-strip REW depends on its importance as a civil engineering structure and the type of ground, as well as the assumed earthquake level and design horizontal seismic intensity. In this experiment, the design horizontal seismic intensity was set to 0.12, considering the constraint of the dimensions of the soil chamber, the importance of the structure, which was set to 1, and the assumed earthquake motion in the design, which was set to be that of a Level 1 Earthquake. The length of the model reinforcement was determined by using a safety factor of F_{sE} = 1.2 in accordance with the performance requirements in the manual for the design and construction of REWs (PWRI, 2014).

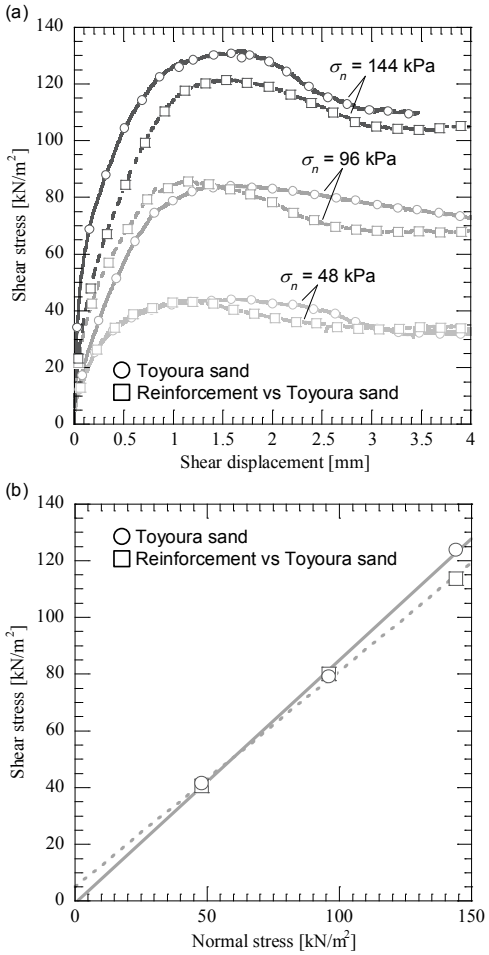

Figure 7. Results of direct shear tests: (a) load-displacement curve and (b) relation between maximum shear stress and normal stress.

Table 2. Comparison of properties of reinforcement between real structure and model.

	Object	Model
Young's modulus: E [kN/m^2]	4.00×105	2.05×108
Width: b [m]	0.060	0.12
Thickness: d [m]	4.00×10-3	1.00×10-2
Moment of area: I [m4]	3.20×10-10	1.00×10-8
Bending stiffness: EI [kN·m^2]	6.40×10-2	2.0
Reinforcement density [mm/m^2]	1.07×102	1.07×102

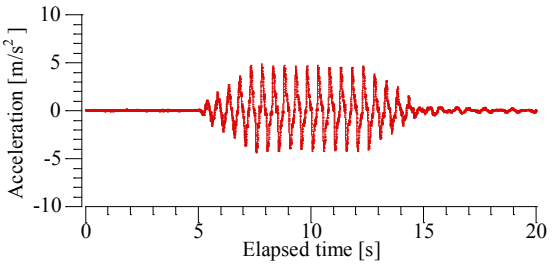

Figure 8. Input wave in the prototype scale: sin wave with 2 Hz and twenty cycles, and magnitude of 5.0 m/s^2 input in Step 5.

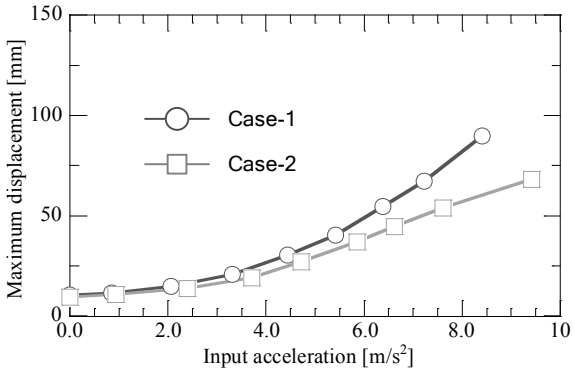

Figure 9. Transition of maximum horizontal wall displacement at each excitation step.

2.5 Input wave

Figure 8 shows an example of the input acceleration in the prototype scale which was measured on the shaking table. The maximum acceleration of the shaking table was increased step by step in increments of 1.0 m/s^2 in order to observe the gradual change in the seismic behavior of the steel-strip REW under repeated earthquake motion. In the experiment, referring to the dynamic centrifuge model experiment on a geotextile REW conducted by Sasaki et al. (2010), the constant state at which the centrifugal acceleration reached 20 G was set as Step 0, and 20 tapered sinusoidal waves with a frequency of 2.0 Hz were applied to the shaking table. The maximum acceleration was in the range of 1.0 m/s^2 to 8.0 m/s^2.

3 SEISMIC BEHAVIOR CHARACTERIZED BY SEGMENTAL WALL PANELS

The experimental results and discussions are summarized in order of the wall displacements and the mechanical relationship among the wall displacements, tensile force of the reinforcement, and the earth pressure acting on the wall panels under and after excitation. The following results were output in the prototype scale.

3.1 Evaluation of wall displacement

Figure 9 presents the maximum horizontal displacement of the wall at each excitation step in Case-1 and Case-2. In comparing these two cases, it can be seen that, at each excitation step, the maximum horizontal displacement remained smaller in Case-2, which has rigid segmental wall panels, than in Case-1, which has a continuous aluminum wall. In addition, the maximum horizontal displacement occurred at the top of the wall in Case-1 and at the second wall panel from the top in Case-2.

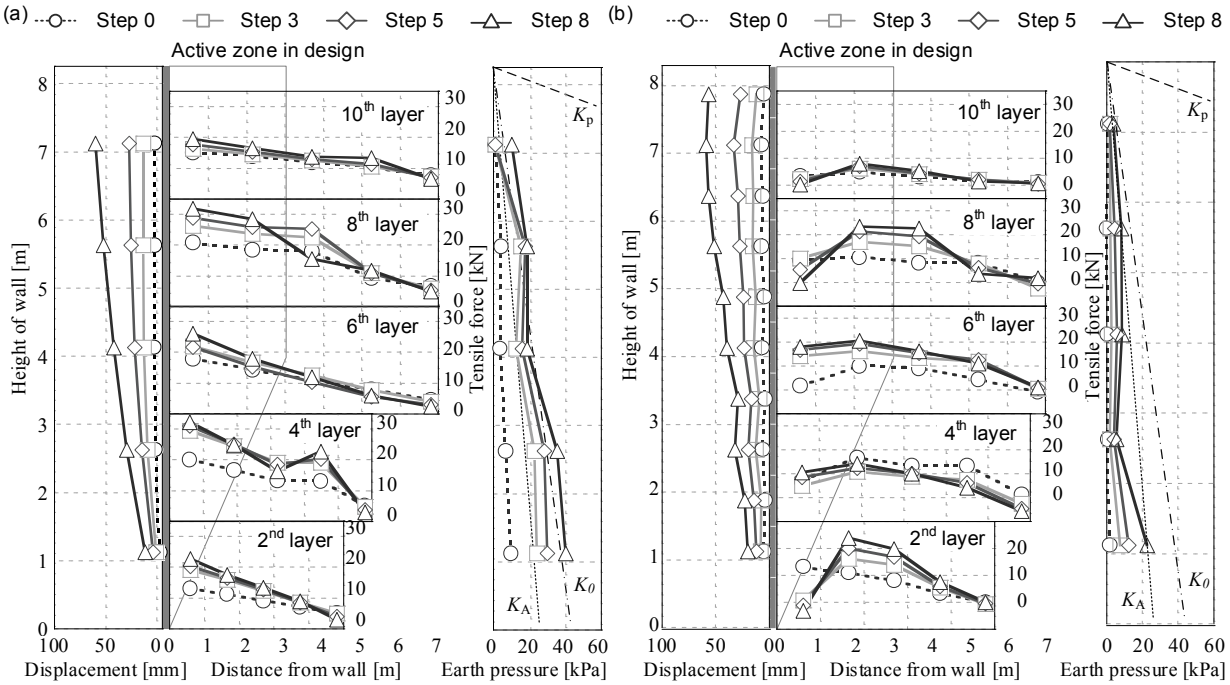

Figure 10. Wall displacement, axial force of reinforcement, and earth pressure acting on wall in Case-2 at Steps 0, 3, 5, and 8 (a) in Case-1 and (b) in Case-2.

The main reason for these trends is thought to be that the same reinforcement length determined by the same factor of safety was applied in both cases, but a small embankment was added in Case-2, which increased the confining pressure and may have slightly suppressed the displacement of the upper wall panels. However, it can be seen from the figure that the REW with segmental wall panels also had high seismic resistance during repeated lateral shaking.

3.2 Wall displacements, tension of reinforcement, and earth pressure

Figures 10 exhibits the relationship of the measured wall displacements, tension distribution of the reinforcements, and earth pressure distribution on the walls between Case-1 and Case-2 after the completion of the Step 0, 3, 5, and 8 excitations.

From the figure, the deformation modes of the wall are seen to be similar in terms of the larger deformation at the top of the wall. On the other hand, in Case-2, the shape of the horizontal displacement distribution of the wall panels was discontinuous after the fourth wall panel from the bottom. Although the maximum horizontal displacement of the wall was smaller in Case-2 than in Case-1, the combined wall by the segmental wall panels (in Case-2) is still unstable against local deformation.

The tension distribution of the reinforcement and the earth pressure distribution in Case-1 were larger than those in Case-2. In addition, the variation in the reinforcement tension due to each excitation step was more amplified in Case-2. The reason why Case-1 had higher reinforcement tension and earth pressure than Case-2 is that the entire wall in Case-1, which had total shear and bending resistance, was able to more strongly support the static and dynamic earth pressure, which was not true for Case-2. Thus, maintaining the earth pressure behind the wall, in turn, increased the restraining pressure acting on the reinforcement. However, in Case-2, since total shear and bending resistance could not be expected, due to little friction between the segmental wall panels, each segmental wall panel bore the earth pressure, resulting in smaller earth pressure on the wall panels and lower confining pressure, which in turn reduced the reinforcement tension.

3.3 Relationship between wall displacement and tension of reinforcement during excitation

To discuss the discontinuity in the wall displacement distribution in Case-2, the mechanical behavior during excitation is analyzed in terms of the relationship between the wall displacement and the tension of the reinforcement. Figure 11 shows the hysteresis loop between the reinforcement tension and the horizontal displacement of the wall or the wall panel. For a comparison based on Case-2, focus is placed on the relationship of the second wall panel from the bottom with high confining pressure and the sixth one from the bottom with medium confining pressure. In Case-1, closer locations are chosen for the measuring points than in Case-2. The tension of the reinforcement was evaluated at the strain gauge just behind the wall or the segmental wall panel.

The plotted values were normalized by the maximum tension and horizontal displacement during excitation. Accordingly, the maximum tension of the reinforcement was obtained from the time history of the measured strain just behind the wall or the wall panel at each excitation step. Similarly, the maximum horizontal displacement was obtained from the measured horizontal displacement of the corresponding wall height or the wall panel at the corresponding height during each excitation step. Focus was placed on two excitation steps with the normalized hysteresis loop: Step 3, the earlier excitation stage with a maximum input acceleration of 3.0 m/s^2, and Step 8, the final excitation stage with a maximum input acceleration of 8.0 m/s^2.

Figure 11 (a) shows that, in Case-1, at the position closer to the second wall panel, where the confining pressure is relatively large, the size of the loop for the horizontal displacement of the wall is larger than that for the tension of the reinforcement during both excitations.

This is because the unity of the reinforcement and the wall was maintained in the region where the confining pressure was large and, as a result, the amount of fluctuation in the wall displacement became larger. In the position closer to the sixth

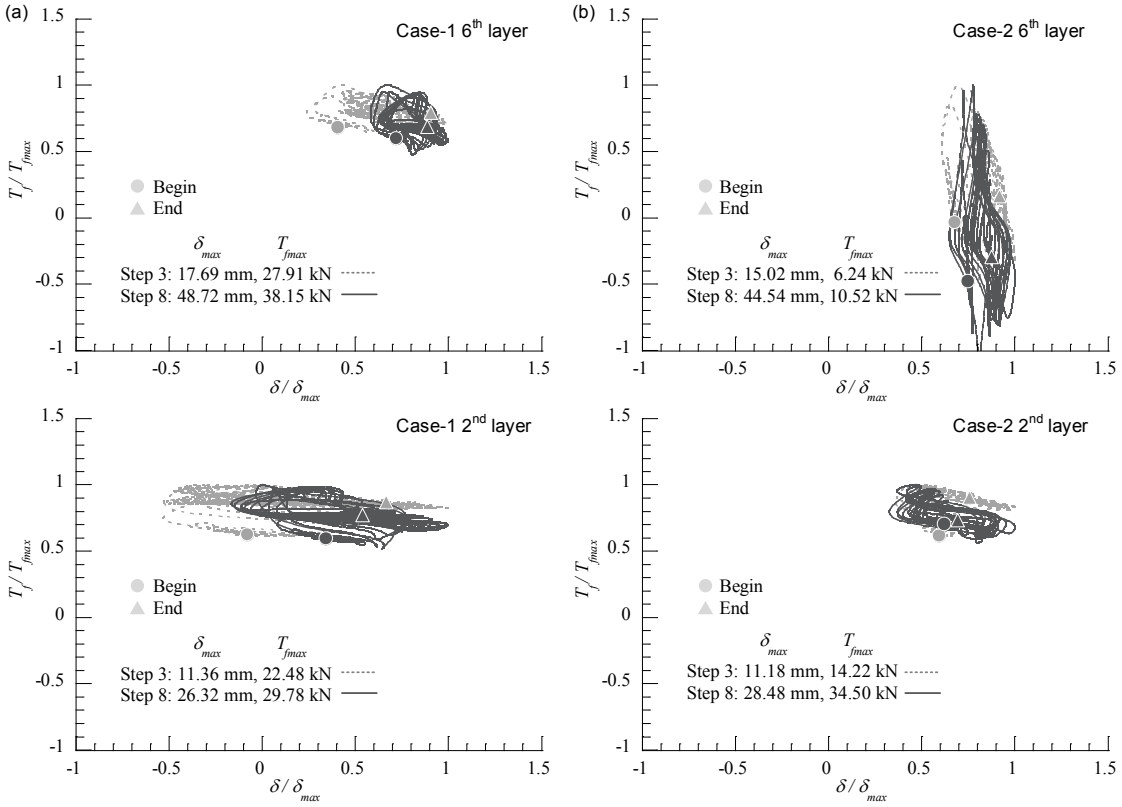

Figure 11. Hysteresis of normalized tensile force and normalized lateral displacement of second wall panels and sixth wall panels in (a) Case-1 and (b) Case-2.

wall panel, as the confining pressure decreased, the tension of the reinforcement and the wall displacement fluctuated at the same level, resulting in a circular shape of the hysteresis loop.

From Figure 11 (b), it can be seen that, in Case-2, the fluctuation in the reinforcement tension and the wall panel's displacement remain close in behavior in the second wall panel from the bottom. However, in the sixth wall panel, the fluctuation in the reinforcement tension becomes perpendicular to the fluctuation in the wall displacement. In other words, the reinforcement tension of the sixth wall panel during excitation was amplified with less influence on the fluctuation of the wall displacement. This implies that the reinforcement tension did not contribute well to the suppression of the wall displacement in the sixth wall panel from the bottom. The confining pressure did not work efficiently in reinforcing the sixth wall panel, and the wall panel behaved freely during excitation. Thus, the difference in seismic behavior of wall panels depends on their positions, and this is considered to be the cause of the discontinuity in the horizontal displacement distribution of REWs composed of segmental wall panels.

4 CONCLUSION

In this study, dynamic centrifuge model tests were conducted to clarify the deformation behavior of a steel-strip reinforced earth wall with segmental wall panels during an earthquake, focusing on the wall structure. In this experiment, the wall model was built of rigid, segmental wall panels and used to simulate the wall structure without total shear or total bending stiffness. From the test results, the deformation mode of the discontinuous wall structure model, brought about by the segmental wall panels, was seen to be similar to that of a continuous wall structure model. However, the horizontal displacement distribution of the discontinuous wall showed discontinuity in terms of the wall displacement distribution at each elevation of the wall during repeated earthquake motion. This was caused by the difference in the relationship among the confining pressure, reinforcement tension, and wall displacement depending on the position of each segmental wall panel.

5 REFERENCES

Ichikawa, S., Suemasa, T., Katada, T., Toyosawa, Y., and Shimada, S. 2006: Dynamic centrifuge model tests on two types of retaining walls reinforced with anchors diddering in wall rigidity, Journal of Japan Society of Civil Engineers (Geosphere Engineering C), Vol. 62, No. 4, pp. 767-779 (in Japanese).

Public Works Research Institute 2014. *Manual for the Design and Construction of Reinforced Earth Wall*, 4th Revised Edition (in Japanese).

Sasaki, T., Nakajima, S., Enomoto, T. 2010. Dynamic centrifuge model tests on segmental geosynthetic reinforced soil retaining walls - Failure mechanisms of segmental GRS walls-, Geosynthetics Engineering Journal, Vol. 25, pp. 169-176 (in Japanese).

Sawamura, Y., Shibata, T. and Kimura, M. 2019: Mechanical role of reinforcement in seismic behavior of steel-strip reinforced earth wall, Soils and Foundations, Vol. 59, No. 3, pp. 710-725.

Tatsuoka, F., 1992. Roles of facing rigidity in soil reinforcing. Keynote Lecture, In; Ochiai, Y., Hayashi, J. Otani, J. (Eds) Proc. Earth Reinforcement Practice, IS-Kyushu '92, Vol. 2, pp. 831−870.